LEAVE THIS PAGE BLANK
DO NOT DELETE THIS PAGE

Integrated Sensing Printhead

Yuxin Lin*
University of Michigan
Taubman College
Dart laboratory

Mania Aghaei Meibodi*
University of Michigan
Taubman College
Dart laboratory

*All authors contributed equally to this research

In-line data collection for Non-Planar 3D Concrete Printing

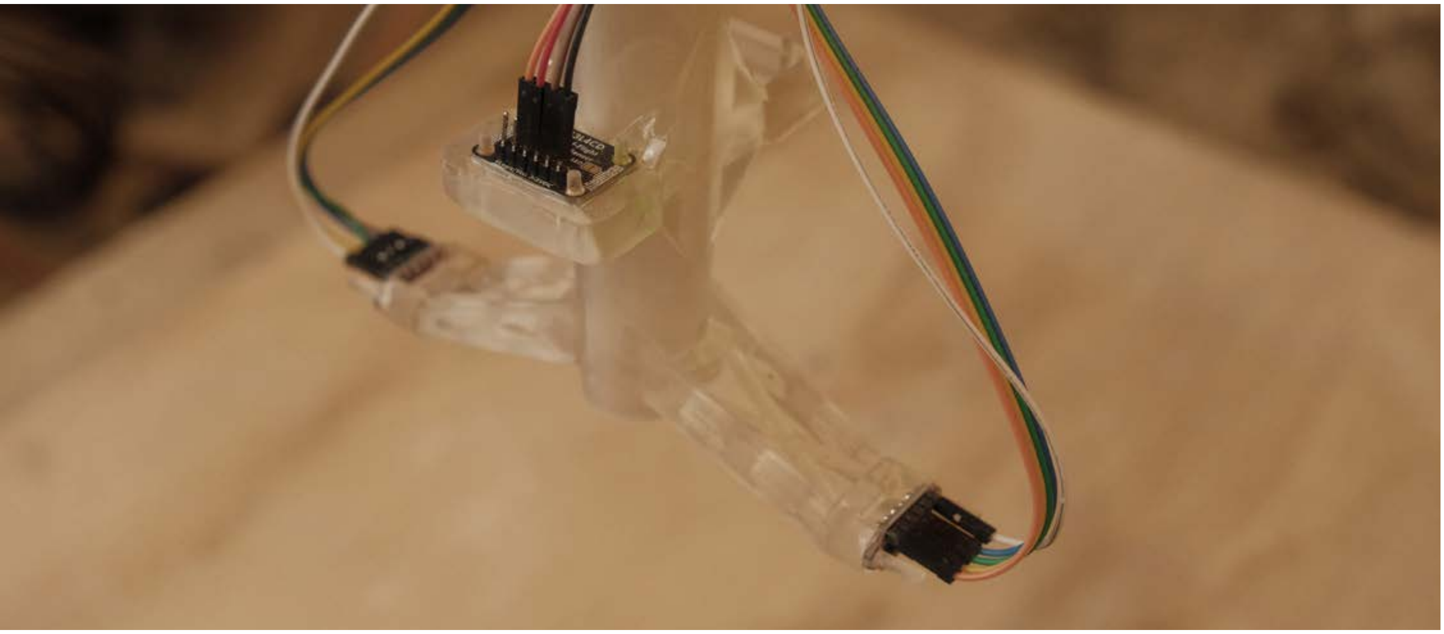

1

1 Configuration of multiple 1D ToF sensors and their integration with the nozzle.

ABSTRACT

Materially optimized building components entail intricate geometries, necessitating the utilization of non-planar printpaths in 3D concrete printing (3DCP). Non-planar robotic 3D concrete printing (NP-3DCP) surpasses the capabilities of traditional planar 3DCP by enabling flexibility in orientation and layer height. In NP-3DCP, the filament's profile undergoes constant change, leading to challenges like unpredictable geometric deformation. To achieve successful and optimal print results, real-time monitoring of critical parameters is essential for live adaptation during the 3DCP process. However, existing research primarily focuses on data collection and monitoring for planar 3DCP with fixed layer height. While some of these methods can be adapted for monitoring NP-3DCP, they overlook the challenges inherent in NP-3DCP, such as variable layer heights requiring continuous extrusion rate adjustment as well as differing deformation conditions. This research will expand the field of data collection for 3DCP by extending the investigation into a data collection method tailored for non-planar 3DCP with curved printpaths. This will be accomplished through the development of a cost-effective measurement tool utilizing multiple 1D Time of Flight (ToF) sensors (Figure 1), along with the formulation of analytical methods and prototyping.

INTRODUCTION

Non-planar 3D concrete printing (NP-3DCP) offers advanced capabilities over traditional planar 3D concrete printing (3DCP), allowing for variations in orientation and layer height. NP-3DCP not only eliminates the need for formwork but also enables the fabrication of complex, materially optimized structural components. Non-planar 3D Printing (NP-3DP) directs the printhead movement across three axes (X, Y, and Z) while dynamically altering the Tool Center Point (TCP) orientation, aligning with the variable layer heights and orientations necessitated by the complex geometries of printed objects (Mitropoulou, Bernhard, and Dillenburger, 2020). Robotic NP-3DP in plastic has shown excellent potential for eliminating the need for scaffolding supports in complex geometries (Dai et al. 2018; Wu et al. 2017), improving surface quality (Song et al. 2017), mechanical performance (Ulu et al. 2015), and feature preservation (Zhang et al. 2015).

Only a limited amount of research, including authors' previous work, has investigated the NP-3DCP technique for manufacturing concrete elements (Anton et al. 2019; Bhooshan et al. 2022; Lin, Bayramvand, and Aghaei Meibodi 2024; Aghaei Meibodi, Lin, and Hao 2024; Kamhawi and Aghaei Meibodi 2024). A critical aspect of NP-3DCP is the precise control of the material extrusion rate, which is essential for matching varying layer heights and ensuring consistent layer width for optimal surface quality (Souza 2022; Bhooshan et al. 2022). Projects such as "Shell Wall" (Lin, Bayramvand, and Aghaei Meibodi 2024), "Branch Wall" and "S-shape structure" (Aghaei Meibodi, Lin, and Hao 2024), "Vertical Modules" (Anton et al. 201) successfully regulated the material deposition rate by pre-programming the various robot print speeds based on the height difference between successive layers, utilizing the following Equation (1).

$$Q = V * W * H \tag{1}$$

Where: Q = material flow rate based on pump speed, V = robot print speed, W = extruded material width, H = filament height (Anton et al. 2021). However, the application of this theoretical model in the actual NP-3DCP process faces several challenges, which are described below:

Geometry inaccuracy: In the conducted "Shell Wall" (Figure 2), "Branch Wall" (Figure 3), and "S-shape structure" studies (Figure 4), geometric precision was achieved by dividing each layer of the printpath with uniform points and then calculating the shortest distance from each point to the previous layer as H to set the V. Through authors' observations, uniformly divided points are not dense enough to accurately gather height variations when the printpath changes unevenly. Additionally, this approach fails to identify overlapping moments when the printpath contains internal conduits.

2

3

4

5

2 "Shell Wall" projects.

3 "Branch Wall" project.

4 "S-shape structures" project.

5 "Vertical Modules" project. (Anton et al. 2019)

Deformation: Uneven deformation of concrete filaments arises from 1) the self-weight and weight of successive layers due to changing geometries, and 2) the gravitational slump of freshly extruded concrete printed on inclines. For example, in the "Vertical Modules" project (Figure 5), this led to collapse through buckling. In the "Branch Wall" and "S-shape structures", gravitational slump caused misalignment of the extruded filament and potential material collapse if it was left without sequential casting intervention.

Extrusion quality: The viscosity of the material in 3DCP changes over time and its sensitivity to environmental factors such as temperature and humidity can cause fluctuating pumping flow rates, resulting in inconsistencies in the printed filament. Additionally, extrusion quality may also be affected by the presence of air gaps originating from various sources, including trapped air within the concrete mixture, inadequate mixing of the concrete, improper nozzle pressure, or extrusion settings.

Some of these challenges are too complex to control or predict during NP-3DCP where the filament's profile is constantly changing. This underscores the need for real-time monitoring of critical parameters to facilitate live adaptation during the 3DCP process for successful and optimal print results. Thus the primary focus of this paper is the development of sensing tools and real-time data collection and analysis methods for NP-3DCP. Our method involves 1) monitoring actual layer height immediately before extrusion to optimize material extrusion rate, 2) monitoring the extruded filament's dimension and position locally to quantify deviations, thereby identifying deformation modes and extrusion anomalies, and 3) investigating the configuration of the sensor tools to acquire data and developing an analytical mode for real-time data analysis. We conducted a series of prototyping experiments to validate the developed tool and method.

LITERATURE REVIEW ON MONITORING METHOD AND TOOLS USED IN 3DCP DATA COLLECTION

Previous studies have explored various non-invasive inline monitoring methods, as well as tools developed and applied in 3DCP, to perform real-time geometrical fidelity inspection and anomaly detection. Furthermore, some of these studies have developed feedback control mechanisms for adjusting concrete printing parameters in real-time.

One approach utilizes a 1D Time of Flight (ToF) distance sensor (Wolfs et al. 2018), which continuously collects 1D point data on the stand-off distance from the nozzle tip to the previously printed layer, measuring and determining the layer height for subsequent deposition. This research has further developed a closed-loop control model that compares the actual layer height with the designed layer height in real-time, enabling dynamic adjustments in the toolhead's z-axis to maintain the intended height.

Computer vision (CV) techniques represent another significant category of layer width monitoring methods. For example, an RGB camera is utilized to capture 2D images of the newly printed layer from a top view, allowing live calculation of layer width through photogrammetry (Kazemian et al. 2019). The over-extrusion or under-extrusion conditions can be detected by comparing the calculated width with the set width. Adjustments are then made to the material flow rate while maintaining a constant robot print speed, ensuring consistent quality of printed layers despite variations in mixture rheology. Similarly, an edge detection-based image processing algorithm applied to 2D images from a monochromatic camera derives the layer width in real-time (Shojaei Barjuei et al. 2022). This derived width information is used to adjust the robot print speed without altering the pump flow rate, ensuring a uniform layer width and improving overall print quality. In another study, two RGB cameras mounted on either side of the printhead acquire 2D images, which are then used for filament width calculation through a deep learning algorithm (Yang et al. 2022). This setup eliminates blind spots when 3DCP follows curved lines, allowing monitoring of filament extrusion in all directions around the nozzle.

Besides monitoring the layer height and layer width separately, the adjustment of material deposition rate necessities accurate simultaneous measurement of layer height, width, and cross-sectional area. Laser triangulation, which uses both the camera and laser projector, captures 2D profile data of the extruded filament, allowing detailed cross-sectional information, including width, height, and area, to be calculated through matrix transformation (Jhun et al. 2024). This precise geometric monitoring enables real-time detection of deviations in filament dimensions, facilitating immediate corrective adjustments and ensuring adherence to designed parameters. In this study, the approach was primarily tested for monitoring the first printed layer rather than for measuring the width and height of individual layers as they are deposited layer by layer.

Some studies investigate the integration of CV with machine learning (ML) techniques to monitor deformation and extrusion anomalies during 3DCP (Davtalab et al. 2022; Rill-García et al. 2022). Here, side profile images of several printed layers have been captured, with ML techniques developed for edge detection or layer segmentation, assessing the condition of interlayer lines and thus detecting any deformations or anomalies in the printing process (Davtalab et al. 2022; Rill-García et al. 2022). Also, the texture of the individual layers has been assessed to monitor the material mix condition (Rill-García et al. 2022). These studies provide both inline and offline monitoring of prints, ensuring early identification of potential issues that could affect print accuracy.

State-of-the-art research on data collection and monitoring primarily focuses on planar 3DCP with fixed layer height. Although some methods can be adapted for NP-3DCP, including monitoring the extrusion quality and horizontal deformation. However, they do not fully address the challenges specific to NP-3DCP. These include maintaining variable layer heights while keeping consistent layer width, which requires continuous adjustment of the extrusion rate, as well as additional deformation issues, such as buckling or gravitational slump. This research will expand

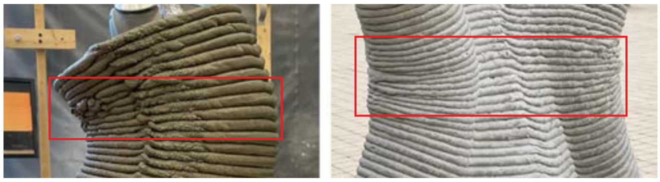

6

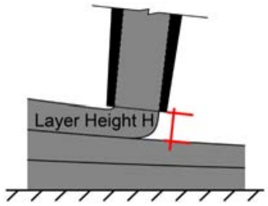

7

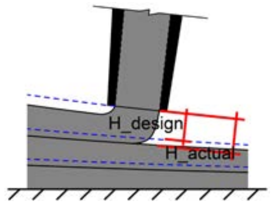

8

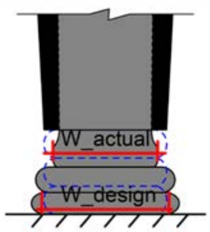

9

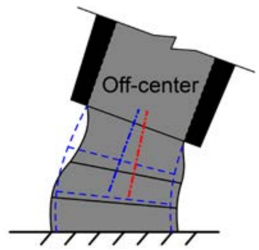

10

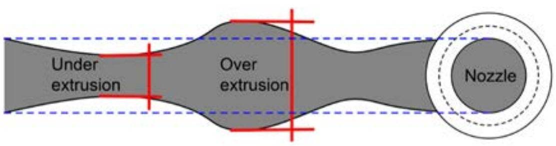

11

6 Maintaining the predetermined variable material extrusion rate still causes excessive material in concave layers and insufficient material in convex layers.

7 The distance between the nozzle tip and the top of the previously extruded layer represents the layer height (H_actual)

8 Horizontal deformation can cause the bottom layer to become wider, reducing the overall print height.

9 As a result of horizontal deformation, the actual layer height for newly extruded material increases, leading to a thinner width during extrusion.

10 Displacement of the newly deposited concrete due to deformation.

11 Two extrusion qualities that are not optimal: under-extrusion and over-extrusion

the investigation into data collection methods for NP-3DCP with curved printpaths. This is achieved by developing a cost-effective measurement tool that uses multiple 1D ToF sensors. This paper will present a design configuration for their placement and the simultaneous data acquisition, as well as further calculation of multiple parameters based on the direct data during the NP-3DCP process.

METHOD

In this study, we have developed a real-time data collection method for robotic NP-3DCP, designed to monitor the actual layer height before extrusion, the width of the newly extruded filament, and its relative position concerning the nozzle, using multiple 1D ToF sensors. The data collected will allow us to compute the optimal material extrusion rate, and to derive geometric derivations for the identification of deformation and extrusion quality.

Monitoring Layer Height for Optimizing Material Extrusion Rate

To ensure geometric fidelity, it is important to determine the filament's variable height (H) accurately. This data will determine the variable velocity (V) of the printhead. An increase in H necessitates a decrease in V, and vice versa. By synchronizing or informing V through H according to Equation (1), we can optimize the material extrusion rate. This adjustment is crucial because, for instance, more material extruded in concave layers can distort geometry and surface quality by squeezing material outward, while less material in convex areas may result in misaligned layers and reduced structural integrity that results in collapse (Figure 6).

The actual layer height (H_actual) can be defined as the distance between the nozzle tip and the top of the previously extruded layer (Figure 7). This measurement needs to be conducted just before the extrusion process, enabling future real-time adjustments to V, and thus facilitating precise regulation of material deposition.

Local Monitoring of Filament Dimensions and Position to Derive Deformation

Horizontal deformation in NP-3DCP may occur due to the self-weight of the material or the weight of subsequently deposited layers, often leading to deviations in the cross-sectional dimensions of the layers (Nguyen-Van et al., 2022). Such deformations typically manifest as the reduced overall height of the print with wider bottom layers before significant structural collapse occurs. To monitor and quantify this consecutive deformation, the collected H_actual is compared to the designed layer height (H_design) of the NP-printpath. Any discrepancy between H_actual and H_design indicates the deformation in the height (Figure 8). Concurrently, monitoring the width of the filament during extrusion provides a secondary validation of deformation. A filament width immediately after extrusion that is smaller than the design suggests increased layer height due to deformation of the previous layers (Figure 9).

Deformation through buckling or the gravitational slump of printing concrete at an angle can cause the displacement of the newly deposited concrete (Chang et al. 2022). Ideally, the centerline of each layer should align with the center of

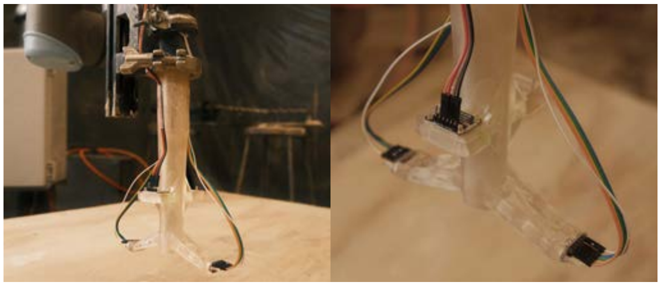

12

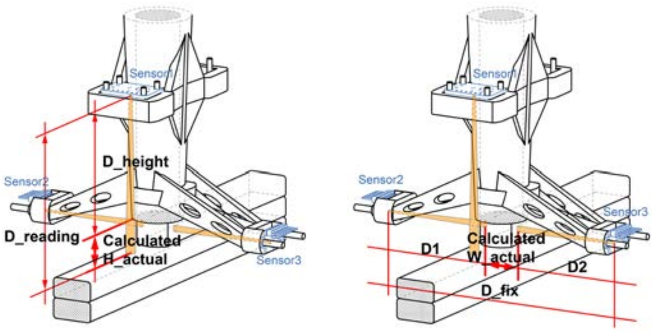

13

12 Sensor configuration and integration with the 3DCP printhead.

13 Direct distances were measured by the sensors to calculate H_actual parameters (left), W_actual parameter and D_difference value (right).

the nozzle tip, however, this type of deformation can cause the newly printed segment to shift off-center of the nozzle (Figure 10). This misalignment can be assessed by monitoring the offset distance between the designed position and the actual position of the filament.

Monitoring Filament Width to Determine Extrusion Quality

The viscosity of concrete is critical for ensuring pumpability and extrudability during the 3DCP process. These two parameters can significantly affect extrusion quality because any variation in them can lead to issues such as over-extrusion or under-extrusion. Over-extrusion occurs when the filament width suddenly exceeds expectations, while under-extrusion happens when the filament width falls short (Figure 11). Using batch-prepared mortar without a continuous mixing pump exacerbates the viscosity variations, which are sensitive to time and environmental conditions, leading to fluctuations in the material flow rate (Q). Additionally, the presence of air gaps or voids within the pipeline system can affect extrusion quality. By monitoring the width of the extruded filament, we can detect these anomalies and ensure optimal extrusion conditions.

Sensor Selection and Configuration for Data Acquisition

Sensor selection and functionality: To conduct accurate two-dimensional measurements of variable filament's profile with a quick response time, this research develops a concrete extrusion printhead equipped with three 1D ToF high-accuracy proximity sensors. Specifically, the VL53L4CD sensor was selected for its precision in the ambient environment, fast-ranging frequency, and short-range measurements. It offers very accurate distance measurements (±3%) starting from a minimum range of 1mm, which is ideal for applications in 3DCP where typical measurements are under 100mm and ranging distances are less than 30mm.

Sensor placement and integration: The strategic placement and integration of sensors are crucial for effectively and accurately monitoring the selected parameters. In the setup of our monitoring system, sensors were strategically positioned around the printhead's nozzle to gather data in both horizontal and vertical manners (Figure 12). Customized holders for these sensors were designed and 3D printed together with the nozzle, ensuring a precise fit and accurate dimension. One ToF sensor was oriented downward, parallel to the toolhead, and maintained a predetermined distance (D_height) from the nozzle tip. Two additional ToF sensors were placed horizontally opposite each other, keeping the same distance from the nozzle tip. The distance (D_fix) between these two sensors was also carefully measured (Figure 13).

Data acquisition of the selected parameters through direct measurements and related calculations: The direct measurements obtained from the sensors are distances, from these distance data we calculated parameters such as the actual width and actual layer height, which are illustrated in Figure 13. To calculate H_actual (Figure 13 left image), we utilize the direct sensor reading (D_reading), which measures the distance from the sensor module to the surface of the faced filament. With D_height being known, H_actual can be derived by subtracting D_height from D_reading as shown in Equation (2). This calculation represents the real-time layer height for the newly extruded filament, which can then be used in Equation (1) to compute the V simultaneously.

$$H\_actual = D\_height - D\_reading \tag{2}$$

Direct readings from two horizontally opposed sensors, D1 and D2, measure the distance from each sensor to the respective side surface of the filament (Figure 13 right image). The actual filament width (W_actual) is calculated by subtracting the sum of these distances from known D_fix, as described by Equation (3). Comparing H_actual and W_actual with the designed height and width facilitates the detection of horizontal deformation.

$$W\_actual = D\_fix - (D1 + D2) \tag{3}$$

Furthermore, sudden and non-smooth changes in W_actual indicate unstable extrusion quality — rapid increases suggest over-extrusion and rapid drops indicate under-extrusion.

Moreover, the differences (D_difference) between D1 and D2 readings help detect displacement in the extruded layers. This displacement, defined in Equation (4), could be indicative of deformation due to buckling or material slumping, as equal readings from D1 and D2 suggest no such deformations

$$D\_difference = D1 - D2 \tag{4}$$

Data Processing and Analysis Methods

Sensors coordination and initial data processing: To acquire the data from Three ToF sensors simultaneously, they are coordinated through the Arduino Uno board using I2C communication. This connection setup involves linking each sensor's VCC (power), GND (ground), SDA (data line), and SCL (clock line) pins to the corresponding pins on the Arduino board. Additionally, each sensor's Xshut pin is connected to an individual digital pin on the Arduino, configured as OUTPUT to manage sensor activation and deactivation for coordinated measurement. The initial processing and transmission of the sensor readings is also conducted in Arduino. This process includes setting the sensors' ranging frequency, executing predefined math- 16
ematical calculations of Equation (2,3,4) to interpret the raw sensor data, and transferring the real-time data to the computer for further analysis.

Data analysis and visualization framework: The raw data collected exhibit non-stationarity, high resolution, and contain noise. To extract value from collected data, a data handling and smoothing framework is developed in VS Code using Python, with integrated functions of MATLAB. The moving average (MA) is utilized to smooth the variations and reduce noise in the time-series data. MA operates by averaging a subset of consecutive data points over a specified window size (N) and replacing each data point with the average of its neighboring points, described as Equation (5).

$$y_n = \frac{1}{N}\sum_{i=0}^{N-1} x_{n-i} \tag{5}$$

This equation calculates the average of the current data point and its N−1 preceding data points, resulting in a smoothed value y_n that represents the local average of the signal within the specified window. As N moves along the time series, it continuously updates the smoothed output based on the current window size of data points. This process effectively attenuates high-frequency noise while preserving the general trend of the sensor readings, thereby outputting smooth distance changes without sharp fluctuations. Concurrently, real-time 2D data visualization is performed by plotting the processed data into a time-series chart, facilitating visual assessment of trends and anomalies.

14

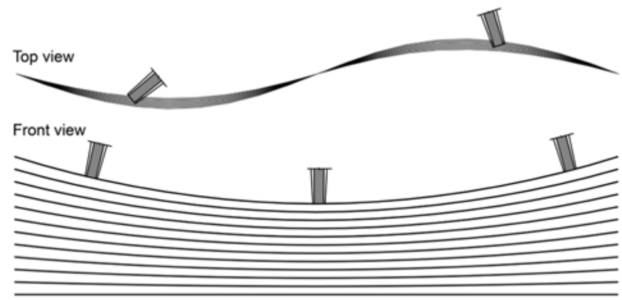

15

14 Actual printing process.

15 Top and front view of the printpath as well as the orientation of printhead.

ANALYSIS AND RESULT

To evaluate the effectiveness and precision of our proposed real-time data collection methods, we conducted a series of 3DCP experiments (Figure 14). This study involved 3DCP along simple curved lines in a non-planar manner, with variable layer heights ranging from 8.1mm to 12.3mm (Figure 15). The collected and calculated numerical data of the extruded concrete filament was analyzed and visualized in real-time.

Real-Time Layer Height Monitoring and Analysis in NP-3DCP

First, we examined the feasibility of monitoring the H_actual during the printing process. Due to the need to turn each sensor on and off to coordinate communication, and considering each sensor's 2ms sleep time as well as the

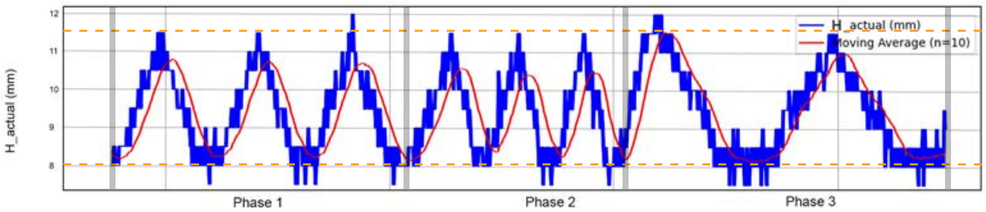

16

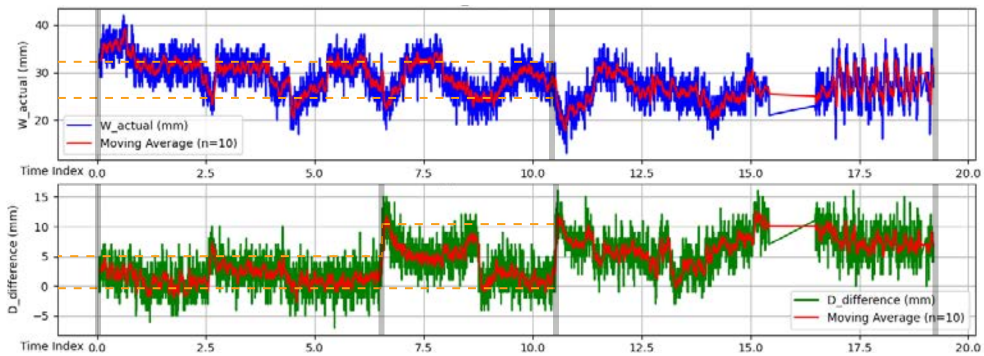

17

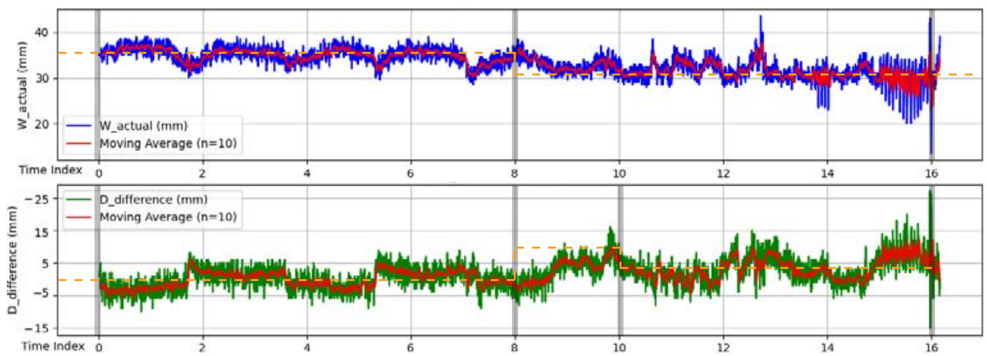

18

19

16 The visualization of collected H_actual data under three different average printing speeds.

17 The visualization of collected W_actual data (up plot) and D_difference data (bottom plot) when horizontal deformation happens.

18 The visualization of collected W_actual data (up plot) and D_difference data (bottom plot) over time when deformation through buckling and material slump happens

19 Horizontal deformation observed during the printing process (left image); material collapse through cumulative buckling or gravitational slump (right image).

inherent response time delay, the minimum measurement interval of the entire system was set at 20ms. Within each period, three sensors operated sequentially, resulting in a system output data rate (ODR) of 50Hz, meaning each sensor provided 50 measurements per second. Given the need for rapid calculations of variable height changes, and based on common practices in similar applications (Proakis and Manolakis 1992), a window size of n=10 was chosen for conducting the MA.

The visualized smoothed data (red line) in Figure 16 could represent the height variations of the printpath throughout differet phases. Variable V was preset concerning the variable H with an average of 100mm/s at phase 1. However, peaks were insufficiently described, showing differences of more than 2mm during phase 1. At an average speed greater than 100mm/s, discrepancies increased to over 3mm in phase 2, resulting in missing geometric details. Conversely, when the average speed was reduced to 50 mm/s during phase 3, the results were optimal, with discrepancies less than 1mm. Thus this average speed was chosen as the reference speed throughout the tests.

The collected H_actual at an average speed of 50mm/s captures the layer height variation from 8.1mm to 11.3mm. Comparing this to the designed layer height values defined by the printpath in Figure 16, which ranges from 8mm to 11.5mm (orange lines), the collected H_actual

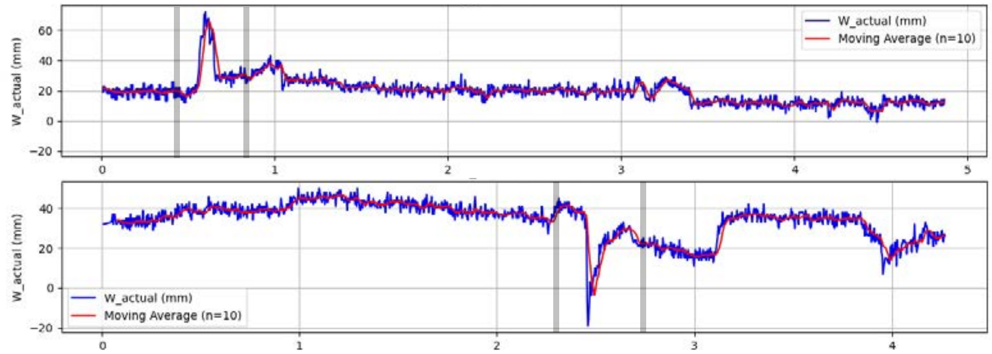

20

21

20 The visualization of collected W_ actual data when over-extrusion (up plot) and under-extrusion (bottom plot) happens.

21 Over-extrusion (left image) and under-extrusion (right image) observed during the printing process.

demonstrates that it is sufficiently accurate to be applicable for adjusting V to achieve optimal extrusion rate.

Deformation Monitoring Through Data Analysis in NP-3DCP
During this test, the variable V was preset in relation to the variable H to ensure consistent layer width in optimal situations and the printhead moved back and forth along the printpath. The up plot in Figure 17 shows the successful monitoring of the newly extruded filament width over time. Notable fluctuations in width measurements were observed, as a general trend of thin width, decreasing from 32mm to 25mm on the two sides. This was followed by a recovery to the initial width of 32mm in the central region. This trend suggests the occurrence of horizontal deformation at the two ends which results in the increased layer height for the new layers (Figure 19 left image). This result is due to the shorter setting time on the two sides than the middle, which is caused by the back-and-forth printpath.

Also, the filament's positional deviations fluctuated within a range of approximately 0mm to 5mm at the beginning, as shown in the bottom plot of Figure 17. This indicates that horizontal deformation does not initially affect the filament position, as it remains centered relative to the nozzle tip. However, cumulative horizontal deformation eventually leads to significant deformation with positional deviations more than 10mm, accompanied by irregular and fluctuating deviations after the onset of this deformation. These deviations result in irreversible printing failures, as evidenced by the irregular variations in actual filament width observed towards the end of the up plot in Figure 17.

In another round of testing, instead of 3D printing back-and-forth, the printhead always started from one side through lead-in and lead-out. This ensured equal setting time for each segment,, effectively minimizing the affect of horizontal deformation. As a result, a relatively stable filament width of approximately 36 mm was achieved, as shown Figure 18 up plot. The deformation through buckling and gravitational slump was then effectively captured, as depicted in Figure 18 bottom plot. This plot visualizes the magnitude of misalignment, showing instances where the actual filament position deviated from being in the center. The pattern of fluctuations indicates that the filament slumps or buckles towards different sides, depending on the printhead's orientation, within a range of ±5 mm for several layers. Subsequent irregular increases in the D_difference indicate moments of substantial misalignment up to 10mm (Figure 18 bottom plot), representing material collapse due to cumulative buckling or gravitational slump (Figure 19 right image). Following this, the plot exhibits irreqular variations, indicating that the material collapse results in irreversible print failure.

Extrusion Quality Monitoring Through Data Analysis
Monitoring filament width during the extrusion process provided critical data also on the flow rate. Figure 20 illustrates the filament width monitoring over time, emphasizing the sudden variations that occurred during the printing process.

During the printing process, while the normal layer width was controlled at around 40mm, Figure 20 up plot shows notable deviations in filament width. There is a sharp increase, indicating over-extrusion (Figure 21 left image). This is possibly due to variations in viscosity. However, the exact reason requires further investigation. Later in Figure 20 bottom plot, the filament width remained relatively stable for a period, with minor fluctuations. Then a significant drop from 40mm to 0mm in filament width is observed, indicating an instance of under-extrusion (Figure 21 right image). Following this, there is an attempt to recover and the filament width displays inconsistently. The air gap was identified through visual inspection which caused this under-extrusion moment.

CONCLUSION

The research presented in this paper highlights the need for real-time data collection and analysis to streamline NP-3DCP by enhancing the accuracy of material deposition. By developing an advanced approach that integrates multiple 1D ToF sensors to monitor critical parameters such as layer height, filament width, and positional deviations, this study enables the identification of deviations, deformation, and extrusion inconsistencies. Experimental results indicate that the proposed monitoring system effectively captures real-time data on actual layer height measurements during the printing of complex, non-planar printpaths. Furthermore, monitoring filament width and positional deviations allows for the early detection and identification of deformation and extrusion issues, thus opening the door for predicting or preventing failure.

Despite these promising results, several areas for further research remain. The current monitoring method is limited to local monitoring of the extruded filament and does not include the overall geometry of the printed structure. Therefore, heterogeneous data collection methods should be investigated to provide a comprehensive monitoring solution. Future work will focus on refining sensor tools development and integration by conducting extensive and large-scale concrete printing experiments. Gathering more data will be critical for validating the system and will likely necessitate the development of more sophisticated analytical methods.

At present, although different sensor readings are collected simultaneously, data analysis is performed separately for different parameters. Future efforts will aim to develop a more comprehensive analysis method to understand the interrelationships among these parameters. This approach has the potential to facilitate the development of real-time feedback control mechanisms based on the collected data, further enhancing the precision and reliability of NP-3DCP.

ACKNOWLEDGEMENTS

We would like to thank Prof. Dr. Branko Kerkez for his valuable expertise and guidance in sensor selection and configuration. We also extend our thanks to Yichun Li for his assistance with the concrete printing process.

REFERENCES

Aghaei Meibodi, Mania, Yuxin Lin, and Hao Chen. 2024. "Hybrid Approaches towards 3D Concrete Printing for Lightweight Reinforced Concrete Structures." https://doi.org/10.24355/DBBS.084-202408140649-0.

Anton, Ana, Lex Reiter, Timothy Wangler, Valens Frangez, Robert J. Flatt, and Benjamin Dillenburger. 2021. "A 3D Concrete Printing Prefabrication Platform for Bespoke Columns." Automation in Construction 122 (103467): 103467. doi:10.1016/j.autcon.2020.103467.

Anton, Ana, Angela Yoo, Patrick Bedarf, Lex Reiter, Timothy Wangler, and Benjamin Dillenburger. 2019. "Vertical Modulations." In ACADIA Proceedings. ACADIA.

Bhooshan, Shajay, Vishu Bhooshan, Alessandro Dell'Endice, Jianfei Chu, Philip Singer, Johannes Megens, Tom Van Mele, and Philippe Block. 2022. "The Striatus Bridge: Computational Design and Robotic Fabrication of an Unreinforced, 3D-Concrete-Printed, Masonry Arch Bridge." Architecture Structures and Construction 2 (4): 521–43. doi:10.1007/s44150-022-00051-y.

Chang, Ze, Hongzhi Zhang, Minfei Liang, Erik Schlangen, and Branko Šavija. 2022. "Numerical Simulation of Elastic Buckling in 3D Concrete Printing Using the Lattice Model with Geometric Nonlinearity." Automation in Construction 142 (104485): 104485. doi:10.1016/j.autcon.2022.104485.

Dai, Chengkai, Charlie C. L. Wang, Chenming Wu, Sylvain Lefebvre, Guoxin Fang, and Yong-Jin Liu. 2018. "Support-Free Volume Printing by Multi-Axis Motion." ACM Transactions on Graphics 37 (4): 1–14. doi:10.1145/3197517.3201342.

Davtalab, Omid, Ali Kazemian, Xiao Yuan, and Behrokh Khoshnevis. 2022. "Automated Inspection in Robotic Additive Manufacturing Using Deep Learning for Layer Deformation Detection." Journal of Intelligent Manufacturing 33 (3): 771–84. doi:10.1007/s10845-020-01684-w.

Jhun, Jihye, Dong-Hyun Lee, Atta Ur Rehman, Seungwoo Kang, and Jung-Hoon Kim. 2024. "Development of a Real-Time Geometric Quality Monitoring System for Extruded Filaments of 3D Concrete Printing Construction." IEEE Access: Practical Innovations, Open Solutions 12: 69981–99. doi:10.1109/access.2024.3401472.

Kamhawi, Abdallah, and Mania Aghaei Meibodi. 2024. "Techniques and Strategies in Extrusion Based 3D Concrete Printing of Complex Components to Prevent Premature Failure." Automation in Construction 168 (105768): 105768. https://doi.org/10.1016/j.autcon.2024.105768.

Kazemian, Ali, Xiao Yuan, Omid Davtalab, and Behrokh Khoshnevis. 2019. "Computer Vision for Real-Time Extrusion Quality Monitoring and Control in Robotic Construction." Automation in Construction 101: 92–98. doi:10.1016/j.autcon.2019.01.022.

Lin, Yuxin, Alireza Bayramvand, and Mania Aghaei Meibodi. 2024. "Towards Lightweight Structure: Coupling Topology Optimization with Non-Planar 3D Concrete Printing." In The 6th International Conference on Computational Design and Robotic Fabrication.

Mitropoulou, Ioanna, Mathias Bernhard, and Benjamin Dillenburger. 2022. "Nonplanar 3D Printing of Bifurcating Forms." 3D Printing and Additive Manufacturing 9 (3): 189–202. doi:10.1089/3dp.2021.0023.

Nguyen-Van, Vuong, H. Nguyen-Xuan, Biranchi Panda, and Phuong Tran. 2022. "3D Concrete Printing Modelling of Thin-Walled Structures." Structures 39: 496–511. doi:10.1016/j.istruc.2022.03.049.

Proakis, John G., and Dimitris Manolakis. 1992. Digital Signal Processing: Principles, Algorithms and Applications. 2nd ed. London, England: Macmillan.

Rill-García, Rodrigo, Eva Dokladalova, Petr Dokládal, Jean-François Caron, Romain Mesnil, Pierre Margerit, and Malo Charrier. 2022. "Inline Monitoring of 3D Concrete Printing Using Computer Vision." Additive Manufacturing 60 (103175): 103175. doi:10.1016/j.addma.2022.103175.

Shojaei Barjuei, E., E. Courteille, D. Rangeard, F. Marie, and A. Perrot. 2022. "Real-Time Vision-Based Control of Industrial Manipulators for Layer-Width Setting in Concrete 3D Printing Applications." Advances in Industrial and Manufacturing Engineering 5 (100094): 100094. doi:10.1016/j.aime.2022.100094.

Song, Hai-Chuan, Nicolas Ray, Dmitry Sokolov, and Sylvain Lefebvre. 2017. "Anti-Aliasing for Fused Filament Deposition." Computer Aided Design 89: 25–34. doi:10.1016/j.cad.2017.04.001.

Souza, Eduardo. 2022. "form Freedom with Mass Customization: Technical Challenges in 3D Printing." ArchDaily. May 5. https://www.archdaily.com/980754/form-freedom-with-mass-customization-technical-challenges-in-3d-printing.

Ulu, Erva, Emrullah Korkmaz, Kubilay Yay, O. Burak Ozdoganlar, and Levent Burak Kara. 2015. "Enhancing the Structural Performance of Additively Manufactured Objects through Build Orientation Optimization." Journal of Mechanical Design (New York, N.Y.: 1990) 137 (11): 111410. doi:10.1115/1.4030998.

Wolfs, Rob J. M., Freek P. Bos, Emiel C. F. van Strien, and Theo A. M. Salet. 2018. "A Real-Time Height Measurement and Feedback System for 3D Concrete Printing." In High Tech Concrete: Where Technology and Engineering Meet, 2474–83. Cham: Springer International Publishing.

Wu, Chenming, Chengkai Dai, Guoxin Fang, Yong-Jin Liu, and Charlie C. L. Wang. 2017. "RoboFDM: A Robotic System for Support-Free Fabrication Using FDM." In 2017 IEEE International Conference on Robotics and Automation (ICRA). IEEE.

Yang, Xinrui, Othman Lakhal, Abdelkader Belarouci, and Rochdi Merzouki. 2022. "Adaptive Deposit Compensation of Construction Materials in a 3D Printing Process." In 2022 IEEE/ASME International Conference on Advanced Intelligent Mechatronics (AIM). IEEE.

Zhang, Xiaoting, Xinyi Le, Athina Panotopoulou, Emily Whiting, and Charlie C. L. Wang. 2015. "Perceptual Models of Preference in 3D Printing Direction." ACM Transactions on Graphics 34 (6): 1–12. doi:10.1145/2816795.2818121.

IMAGE CREDITS

Figure 5: Anton et al. 2019
All other drawings and images by the authors.

Yuxin Lin is a Ph.D. student at the Digital Architecture Research & Technologies (DART Lab) within the Taubman College of Architecture and Urban Planning at the University of Michigan. His research focuses on advancing Robotic 3D Concrete Printing techniques alongside real-time control through the collection of live data. This work aims to facilitate the manufacturing of optimized and high-definition concrete components for use in the construction and building sectors.

Mania Aghaei Meibodi is an Assistant Professor of Architecture at Taubman College of Architecture and Urban Planning at the University of Michigan. She is now teaching in Master of Science in Digital and Material Technologies and is actively involved in expanding the Ph.D. program. Aghaei Meibodi has been a leader in developing novel computational design and fabrication methods suitable for large scale manufacturing in building industry. She also leads the DART laboratory, where her team innovates integrative computational design methods with robotic construction and 3D printing to tackle real-world construction challenges.